



HAL
open science

Auger spectroscopy thermodesorption of Sb on Si_{1-x}Gex layers grown on Si(1 0 0) substrates

A. Portavoce, F. Bassani, A. Ronda, I. Berbezier

► To cite this version:

A. Portavoce, F. Bassani, A. Ronda, I. Berbezier. Auger spectroscopy thermodesorption of Sb on Si_{1-x}Gex layers grown on Si(1 0 0) substrates. *Surface Science: A Journal Devoted to the Physics and Chemistry of Interfaces*, 2002. hal-02393648

HAL Id: hal-02393648

<https://amu.hal.science/hal-02393648>

Submitted on 4 Dec 2019

HAL is a multi-disciplinary open access archive for the deposit and dissemination of scientific research documents, whether they are published or not. The documents may come from teaching and research institutions in France or abroad, or from public or private research centers.

L'archive ouverte pluridisciplinaire **HAL**, est destinée au dépôt et à la diffusion de documents scientifiques de niveau recherche, publiés ou non, émanant des établissements d'enseignement et de recherche français ou étrangers, des laboratoires publics ou privés.

Auger spectroscopy thermodesorption of Sb on $\text{Si}_{1-x}\text{Ge}_x$ layers grown on Si(1 00) substrates

A. Portavoce ^{a,b}, F. Bassani ^{a,*}, A. Ronda ^a, I. Berbezier ^a

^a CRMC2-CNRS, Ctr. de Recherche sur les Mecanismes de la Croissance Cristalline, Campus de Luminy, Case 913, 13288 Marseille cedex 9, France

^b L2MP-CNRS, Av. escadrille Normandie-Niemen, Case 151, 13397 Marseille cedex 13, France

Received 12 October 2001; accepted for publication 23 July 2002

Abstract

Desorption of Sb from $\text{Si}_{1-x}\text{Ge}_x$ layers ($x = 0, 0.05, 0.1, 0.2, 1$) grown by molecular beam epitaxy (MBE) on Si(1 00) substrates is investigated using Auger electron spectroscopy thermodesorption (TD-AES). Sb desorption process on $\text{Si}_{1-x}\text{Ge}_x$ is well described by a first-order reaction. No extra TD-AES peaks are observed on $\text{Si}_{1-x}\text{Ge}_x$ compared to Si. For 1 ML of Sb coverage the TD-AES peak shifts to lower temperature when Ge bulk concentration increases. The Sb monolayer desorbs at 801, 752, 740, 715, and 706 °C for $x = 0, 0.05, 0.1, 0.2$ and 1, respectively. We explain the non-linear decrease of the Sb desorption energy when x increases by the strong Ge surface segregation during the MBE growth of $\text{Si}_{1-x}\text{Ge}_x$ layers, resulting in an almost pure Ge surface even for low x .

© 2002 Elsevier Science B.V. All rights reserved.

Keywords: Antimony; Silicon; Germanium; Thermal desorption; Auger electron spectroscopy; Molecular beam epitaxy

1. Introduction

Understanding of group-V elements adsorption on IV–IV heterostructures is of potential interest for doping and for surfactant-mediated epitaxial growth of these structures. In particular, antimony (Sb) is the usual n-type dopant used in silicon (Si) molecular beam epitaxy (MBE). To improve the control of its doping profile in Si-based heterostructures, studies on Sb diffusion, surface segregation and desorption have to be performed. Despite the numerous works describing and study-

ing these phenomena for Si [1–4], very few studies have been realized for SiGe although the fabrication of abrupt junctions is of great interest for possible electronic and optoelectronic device applications. In the latter case, the existing studies mainly concern Sb bulk diffusion [5] and surface segregation [6] in SiGe, but to our knowledge there has not been a report on Sb desorption from SiGe surfaces up to now. In addition, such studies could be also important in clarifying the Sb surfactant effect on the growth of SiGe layers. Indeed Sb was found to modify the growth mode of Ge on Si by delaying the onset of three-dimensional clustering in Stranski–Krastanov growth [7]. In addition, people have recently used Sb to increase the density and reduce the size of Ge islands [8,9].

* Corresponding author. Tel.: +33-662922872; fax: +33-491418916.

E-mail address: bassani@crmc2.univ-mrs.fr (F. Bassani).

Regarding Sb desorption, Metzger and Allen [10] have evidenced that its order is unity on Si and that Si(111) and Si(100) orientations exhibit identical behaviour. Two distinct peaks of Sb desorption are observed: one at low temperature corresponding to high Sb coverage and one at high temperature corresponding to a coverage lower than 0.5 or 1 ML for Si(100) and Si(111), respectively. The high temperature peak results from the Sb–Si interaction while the low temperature peak is attributed to the Sb–Sb interaction. A similar situation is encountered for the Ge(100) surface, for which Chan and Altman [11] have recently observed three Sb desorption peaks: a high temperature peak at 707 °C attributed to the Sb–Ge bond breaking, a low temperature peak at 277 °C corresponding to Sb–Sb bonding, and a third peak observed at 817 °C being probably due to desorption of incorporated Sb atoms which need to diffuse to the surface before desorbing.

In this paper, we report new results concerning the Sb surface desorption from $\text{Si}_{1-x}\text{Ge}_x$ layers grown by MBE on Si(100) substrates using Auger electron spectroscopy thermodesorption (TD-AES). We study the evolution of the high temperature desorption peak (desorption of 1 ML of Sb) with the Ge concentration of several SiGe layers. Sb monolayer (ML) desorption temperature is found to decrease when Ge bulk concentration (x) increases and the corresponding desorption energies decrease exponentially up to the value for a pure Ge surface. This behaviour is explained by the strong surface segregation of Ge during the growth, leading to a pure Ge surface even for low Ge bulk concentration.

2. Experimental

Samples were grown in a Riber MBE chamber with a base vacuum in the 10^{-11} Torr range and a pressure during deposition in the 10^{-10} Torr range. Si and Ge were evaporated by means of an electron gun evaporator monitored by an INFICON Sentinel III deposition controller and an effusion cell with a pyrolytic boron nitride crucible, respectively. Sb was sublimated using a standard effusion cell. Si and $\text{Si}_{1-x}\text{Ge}_x$ growth rates for dif-

ferent composition of Ge were calibrated by reflection high-energy electron diffraction (RHEED) oscillations observed at low temperature on Si(111) substrates. Typical Si and Ge growth rates were 0.375 Å/s and varied from 0.02 to 0.094 Å/s, respectively. Sb calibration was done using the surface reconstruction change from the Si(100)-(2 × 1) pattern to the (1 × 1) pattern at a Sb coverage of 1 ML [12]. Nominal Sb flux rate was estimated to be 2.2×10^{13} molecules $\text{cm}^{-2} \text{s}^{-1}$. Substrate temperatures were measured with a thermocouple fixed on the backside of the sample holder and complimented by infrared pyrometry. Various eutectic points in the investigated temperature range were used to calibrate the temperature given by the thermocouple. The Si substrate cleaning procedure consisted of an in situ thermal annealing at 1200 °C for 1.5 min to desorb the native oxide, followed by a 34 nm thick Si layer grown at 750 °C. Sample surface quality was checked by RHEED: all sample surfaces were flat and reconstructed ((2 × 1) on Si(100) and (7 × 7) on Si(111)). Subsequently $\text{Si}_{1-x}\text{Ge}_x$ layers with $x = 0.05, 0.1, 0.2,$ and 1 were grown at 630 °C and finally capped with 1 ML of Sb at 400 °C.

Five layers were epitaxially grown on Si(100) substrates: a Si layer, three 28 nm thick $\text{Si}_{1-x}\text{Ge}_x$ layers with $x = 0.05, 0.1$ and 0.2 respectively and a 3 ML thick Ge layer. Note that the thickness of the Ge layer is strongly reduced in order to avoid 3D growth or nucleation of dislocations. A Si layer was also grown on a Si(111) substrate. After the deposition of 1 ML of Sb, samples were transferred into the analysis chamber equipped with Auger electron spectroscopy (AES). Auger spectra were systematically performed before heating the sample. As can be seen on Fig. 1, no observable contamination of the surface by either C or O was detected. Si (92 eV) and Ge (1147 eV) Auger intensities (peak-to-peak height) for each sample are reported in Table 1. These values will be used later in order to estimate the Ge surface segregation. Then a linear temperature ramp with a heating coefficient $\beta = 0.5$ °C/s was applied to the samples starting from $T_0 = 240$ °C. During this procedure, adsorbed Sb atoms can desorb at temperatures which depend on their surface binding energy. Here, determination of the amount of Sb desorbed

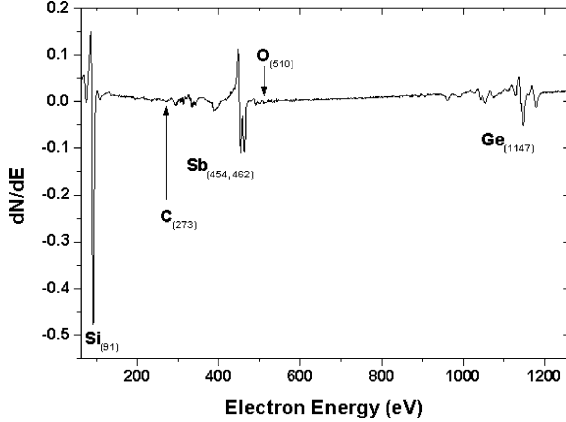


Fig. 1. Auger electron spectroscopy spectrum of a 28 nm thick $\text{Si}_{0.8}\text{Ge}_{0.2}$ layer grown on Si(100) substrate and capped with 1 ML of Sb.

Table 1
Auger intensity (peak-to-peak height) of the Si (92 eV) and Ge (1147 eV) peaks for $\text{Si}_{1-x}\text{Ge}_x$ layers^a

$\text{Si}_{1-x}\text{Ge}_x$	$x = 0$	$x = 0.05$	$x = 0.1$	$x = 0.2$	$x = 1$
Si intensity	1.15	0.904	0.791	0.601	0.548
Ge intensity	0	0.00559	0.0351	0.1	0.0871

^a The incident electron energy was equal to 3.2 keV.

is made by analysing the Sb quantity remaining on the surface ($N(t)$) using AES [13]. More precisely, $N(t)$ is measured from the (peak-to-peak) height of the derivative of the Sb $\text{M}_5\text{N}_{4.5}\text{N}_{4.5}$ peak. During Sb desorption, the corresponding signal decreases whereas the Si and Ge signals increase, since they are less screened by Sb. This desorption experiment can be expressed by the well-known equations [14]:

$$\frac{dN(t)}{dt} = -K_d \times N(t)^n \quad (1)$$

$$K_d = K_0 \times \exp\left(-\frac{E_d}{kT}\right) \quad (2)$$

$$T = T_0 + \beta \times t \quad (3)$$

where $N(t)$, K_d , K_0 , E_d and n are defined as the Sb surface coverage measured by AES, the rate constant of desorption, the frequency factor, the de-

sorption energy and the order of the reaction, respectively. At the temperature of the Sb monolayer desorption maximum (T_p) the second derivative of $N(t)$ vanishes, which leads to:

$$\frac{E_d}{kT_p^2} = n \times N(t)^{n-1} \times \frac{K_0}{\beta} \times \exp\left(-\frac{E_d}{kT_p}\right) \quad (4)$$

This last equation allows us to calculate E_d when K_0 and T_p are known.

3. Results

First, we confirm that Sb is more strongly bound to the Si(100) surface than to the Si(111) surface [10]. Indeed, the Sb monolayer was found to desorb at 801 °C on Si(100) and at 752 °C on Si(111). Moreover the asymmetric TD-AES signal found on both surfaces reveals a first-order reaction ($n = 1$). Using Eq. (4) and taking K_0 from the literature, activation energies (E_d) were calculated. Concerning the Sb interaction with the Si(111) surface, using $K_0 = 4 \times 10^{11} \text{ s}^{-1}$, one finds $E_d = 2.73 \text{ eV}$, in better agreement with the values found by Andrieu and Arnaud d'Avitaya [15] ($E_d = 2.65 \pm 0.15$) and Ladeveze et al. [13] ($E_d = 2.70 \pm 0.05 \text{ eV}$) than that of Metzger and Allen [10,16] ($E_d = 2.46 \text{ eV}$). On Si(100) Metzger and Allen [10] measured $K_0 = 2.0 \times 10^{12} \text{ s}^{-1}$ and $E_d = 3.05 \text{ eV}$. Taking the same value of K_0 and $T_p = 801 \text{ °C}$ Eq. (4) gives $E_d = 3.01 \text{ eV}$ which is in good agreement with their result.

Fig. 2 shows the Sb TD-AES spectra obtained after derivation of the AES signal of four $\text{Si}_{1-x}\text{Ge}_x$ layers ($x = 0, 0.05, 0.2$ and 1) grown on Si(100) substrates subsequently covered by 1 ML of Sb. For sake of clarity, the spectrum for $x = 0.1$ is not presented in this figure. Note first that whatever the Ge composition of the layers, there is only one desorption peak observed, which evidences the existence of a single type of Sb adsorption state. This can be achieved by assuming a homogeneous Ge composition in the surface layer. In this case a linear variation of the adsorption energy can be expected, defined as:

$$E_d(S) = xE_d^{\text{Ge}}(S) + (1-x)E_d^{\text{Si}}(S) \quad (5)$$

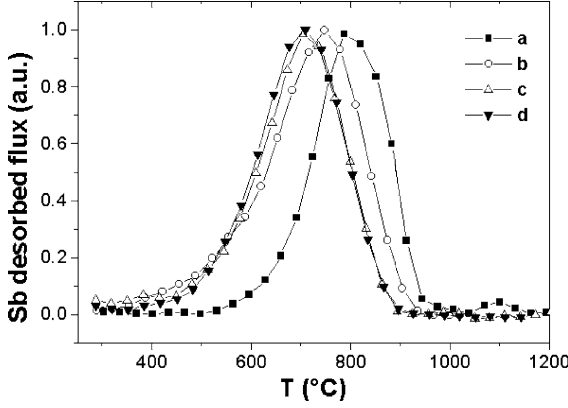


Fig. 2. TD-AES spectra of 1 ML of Sb deposited on four $\text{Si}_{1-x}\text{Ge}_x$ layers ($x =$ (a) 0, (b) 0.05, (c) 0.2, (d) 1) grown by MBE on Si(1 0 0) substrates. All the spectra are recorded under same experimental conditions and obtained after the derivation of the AES signal.

where $E_d(S)$ is the adsorption energy of Sb in the state S (a given adsorption configuration). All spectra exhibited the same asymmetric shape indicating a first order reaction. The Sb desorption for the 3 ML thick Ge sample is found to occur at 706 °C, which is very close to the value found by Chan and Altman (707 °C) for a Ge(1 0 0) substrate. The latter result suggests that the stress induced by the epitaxy of Ge on Si(1 0 0) does not influence significantly the Sb desorption. Moreover, the TD-AES peak is found to shift to lower temperature when the Ge bulk content increases, which confirms that the binding energy of Sb decreases when the Ge composition increases. The difference between Sb ML desorption temperatures from Si and from Ge ($\Delta T = T_p^{\text{Si}} - T_p^{\text{Ge}} = 95$ °C) is in good agreement with previous theoretical

calculations performed by Jenkins and Srivastava [17], indicating that adsorbed Sb atoms are more strongly bound to the Si surface than to the Ge surface (Sb–Si bonds are 0.1 eV stronger than Sb–Ge bonds). Fig. 2 also shows that the TD-AES peak does not shift linearly with the Ge layer composition and for samples with $x = 0.2$ and 1, the peaks are almost superimposable. Assuming a constant value $K_0 = 2.0 \times 10^{12} \text{ s}^{-1}$, Sb desorption energies for the five samples were calculated. K_0 , which is the entropic term of the desorption, is assumed to be constant since only one peak of desorption is observed for all the spectra, corresponding to one configuration of adsorption. The variation of the desorption energy is interpreted as a bonding energy variation for a given configuration of adsorbed Sb atoms. The obtained values of E_d and the corresponding desorption lifetime ($\tau = 1/K_d$) for two temperatures, 550 and 750 °C demarcating the usual MBE growth temperature domain, are reported in Table 2. Fig. 3 shows the Sb desorption rate constant at 750 °C and corresponding activation energies versus the Ge bulk concentration for the investigated samples. K_d and E_d logarithmically increases and decreases respectively when x increases. This behaviour can be explained by considering the surface segregation of Ge which occurs during the growth of SiGe layers [18,19], before the deposition of Sb. The three main driving forces of the segregation phenomenon are the difference in surface energy ($\gamma^{\text{Si}}/\gamma^{\text{Ge}} = 1.25$), the difference in size ($r_{\text{Ge}} - r_{\text{Si}} = 0.0269 \text{ \AA}$) between the components, and their ability to intermix in the bulk (mixing energy) [20]. The two first driving forces promote a strong surface segregation of Ge in Si.

Table 2

TD-AES peak temperature (T_p) and corresponding desorption energies (E_d) of Sb from $\text{Si}_{1-x}\text{Ge}_x$ layers having various Ge composition (x) grown by MBE on Si(1 0 0) substrates

x	x_s	T_p (°C)	E_d (eV)	K_d (s^{-1})		τ (s)	
				$K_0 = 2 \times 10^{12} \text{ s}^{-1}$	$T = 550 \text{ °C}$	$T = 550 \text{ °C}$	$T = 750 \text{ °C}$
0	0	801	3.01	7.54×10^{-7}	3.01×10^{-3}	1.33×10^6	332
0.05	0.18	752	2.87	5.43×10^{-6}	1.49×10^{-2}	1.84×10^5	67.1
0.1	0.37	740	2.83	9.54×10^{-6}	2.32×10^{-2}	1.05×10^5	43.1
0.2	0.81	715	2.76	2.56×10^{-5}	5.13×10^{-2}	3.91×10^4	19.5
1	1	706	2.74	3.39×10^{-5}	6.44×10^{-2}	2.95×10^4	15.5

Values of the Sb desorption rate constant (K_d) and the Sb residence lifetime (τ) are given for two different temperatures. x_s is the Ge composition of the surface of the $\text{Si}_{1-x}\text{Ge}_x$ layers measured by AES.

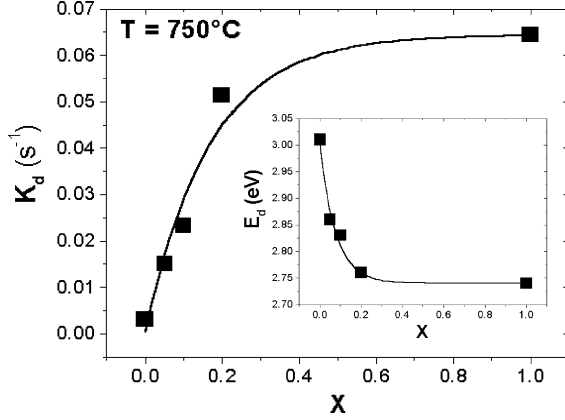


Fig. 3. Desorption rate constant (K_d) as a function of the Ge content (x) for the investigated samples. Inset shows the variation of the corresponding Sb desorption energy (E_d).

The Ge surface segregation has been estimated for each sample using Auger intensity of Si (92 eV) and Ge (1147 eV) transitions obtained before the temperature ramp. For an homogeneous film containing n atomic layers (for the surface $n = 1$), the measured Auger intensity (I_n) can be given by the following formula [21]:

$$I_n = I_1 + \alpha I_1 + \alpha^2 I_1 + \dots + \alpha^{n-1} I_1 = \frac{1 - \alpha^n}{1 - \alpha} I_1 \quad (6)$$

$$\text{with } \alpha = \exp\left(\frac{-1}{\lambda \cos(\omega)}\right) \quad (7)$$

where α is the attenuation parameter, λ is the inelastic mean free path (IMFP) of electrons (in monolayer units) and ω is the emission angle of Auger electrons. The IMFP of Si (92 eV) and Ge (1147 eV) transitions are 0.47 and 1.68 nm respectively [22], which gives $\alpha_{\text{Si}} = 0.65$ and $\alpha_{\text{Ge}} = 0.88$ in our experimental conditions ($\omega = 48^\circ$).

The Ge segregation is assumed to take place only in the surface monolayer, and the sub-surface layer probed by AES is assumed to be a homogeneous $\text{Si}_{1-x}\text{Ge}_x$ layer (IMFP \ll $\text{Si}_{1-x}\text{Ge}_x$ layer thickness). Then the ratio between the AES intensity of Ge (I^{Ge}) and Si (I^{Si}) peaks measured on a same sample can be expressed as:

$$\frac{I^{\text{Ge}}}{I^{\text{Si}}} = \frac{I_{\text{seg}}^{\text{Ge}}(2) + I_{\text{SiGe}}^{\text{Ge}}(3 \rightarrow \lambda_x^{\text{Ge}})}{I_{\text{seg}}^{\text{Si}}(2) + I_{\text{SiGe}}^{\text{Si}}(3 \rightarrow \lambda_x^{\text{Si}})} \quad (8)$$

$I_{\text{seg}}^{\text{Ge}}(2)$ and $I_{\text{seg}}^{\text{Si}}(2)$ are the respective AES intensities of Ge and Si coming from the surface monolayer, covered by 1 ML of Sb, in which Ge atoms have segregated. $I_{\text{SiGe}}^{\text{Ge}}(3 \rightarrow \lambda_x^{\text{Ge}})$ and $I_{\text{SiGe}}^{\text{Si}}(3 \rightarrow \lambda_x^{\text{Si}})$ are the respective AES intensities of Ge and Si coming from the $\text{Si}_{1-x}\text{Ge}_x$ sub-surface layer delimited by the atomic plan number 3 and the last plan probed (λ_x^{Ge} and λ_x^{Si} are the IMFP of electrons emitted by Ge and Si respectively in a homogeneous $\text{Si}_{1-x}\text{Ge}_x$ film). The atomic fraction of an element in an homogeneous alloy can be measured by comparing AES signals emitted by the alloy and by a pure layer of this element with same thickness. Then if one defines x_s and x as the Ge concentration in the surface monolayer (covered by 1 Sb ML) and in the sub-surface layer, it comes:

$$\begin{aligned} \frac{I_{\text{seg}}^{\text{Ge}}(2)}{I_{\text{Ge}}^{\text{Ge}}(2)} &= x_s, & \frac{I_{\text{seg}}^{\text{Si}}(2)}{I_{\text{Si}}^{\text{Si}}(2)} &= 1 - x_s \\ \frac{I_{\text{SiGe}}^{\text{Ge}}(3 \rightarrow \lambda_x^{\text{Ge}})}{I_{\text{Ge}}^{\text{Ge}}(3 \rightarrow \lambda_x^{\text{Ge}})} &= x, & \frac{I_{\text{SiGe}}^{\text{Si}}(3 \rightarrow \lambda_x^{\text{Si}})}{I_{\text{Si}}^{\text{Si}}(3 \rightarrow \lambda_x^{\text{Si}})} &= 1 - x \end{aligned} \quad (9)$$

with $I_{\text{Ge}}^{\text{Ge}}(2)$ and $I_{\text{Si}}^{\text{Si}}(2)$ the AES intensity emitted by pure Ge and Si surface monolayers covered by 1 ML Sb respectively and $I_{\text{Ge}}^{\text{Ge}}(3 \rightarrow \lambda_x^{\text{Ge}})$ and $I_{\text{Si}}^{\text{Si}}(3 \rightarrow \lambda_x^{\text{Si}})$ the respective AES intensity emitted by a pure Ge layer and a pure Si layer located between the atomic plane number 3 and λ_x . Then Eqs. (8) and (9) give:

$$\begin{aligned} \frac{I^{\text{Ge}}}{I^{\text{Si}}} &= \frac{x_s I_{\text{Ge}}^{\text{Ge}}(2) + x I_{\text{Ge}}^{\text{Ge}}(3 \rightarrow \lambda_x^{\text{Ge}})}{(1 - x_s) I_{\text{Si}}^{\text{Si}}(2) + (1 - x) I_{\text{Si}}^{\text{Si}}(3 \rightarrow \lambda_x^{\text{Si}})} \quad (10) \\ x_s &= \frac{\frac{I^{\text{Ge}}}{I_{\text{Si}}^{\text{Si}}(2)} [I_{\text{Si}}^{\text{Si}}(2) + (1 - x) I_{\text{Si}}^{\text{Si}}(3 \rightarrow \lambda_x^{\text{Si}})] - x I_{\text{Ge}}^{\text{Ge}}(3 \rightarrow \lambda_x^{\text{Ge}})}{\left(\frac{I^{\text{Ge}}}{I_{\text{Si}}^{\text{Si}}(2)} I_{\text{Si}}^{\text{Si}}(2) + I_{\text{Ge}}^{\text{Ge}}(2)\right)} \quad (11) \end{aligned}$$

For the calculation of the IMFP of electrons having an energy E in $\text{Si}_{1-x}\text{Ge}_x$ (λ_x^E) a linear relation between Si and Ge is used:

$$\lambda_x^E = (1 - x) \frac{\lambda_{\text{Si}}^{\text{Si}}}{E_{\text{Si}}} E + x \frac{\lambda_{\text{Ge}}^{\text{Ge}}}{E_{\text{Ge}}} E \quad (12)$$

with $\lambda_{\text{Si}}^{\text{Si}} = 3.46$ ML and $\lambda_{\text{Ge}}^{\text{Ge}} = 12$ ML. Using Eq. (6), the AES signals measured for the pure Si sample and the 3 ML thick pure Ge layer allow the calculation of $I_{\text{Si}}^{\text{Si}}(2)$ and $I_{\text{Ge}}^{\text{Ge}}(2)$, which permit the calculation of $I_{\text{Si}}^{\text{Si}}(3 \rightarrow \lambda_x^{\text{Si}})$ and $I_{\text{Ge}}^{\text{Ge}}(3 \rightarrow \lambda_x^{\text{Ge}})$ for

each sample ($x = 0.05, 0.1, 0.2$). Then using Eq. (11), the Ge concentration located at the surface of the samples was measured and reported in Table 2. The Ge LMM AES cross-section is 2–3 times less intense (with a 3 keV incident energy electron) than the Si LMM signal, reducing the intensity ratio to $\sim 1\%$ for the bulk signals. A Ge concentration of 5% in Si is close to the limit of sensitivity of AES, so we have neglected the signal coming from the sub-surface ($n > 2$) with respect to the signal coming from the surface ($n = 2$) for the sample with $x = 0.05$:

$$x_s^{0.05} \approx \frac{\frac{I_{\text{Si}}^{\text{Ge}}}{I_{\text{Si}}^{\text{Si}}} [I_{\text{Si}}^{\text{Si}}(2) + (0.95)I_{\text{Si}}^{\text{Si}}(3 \rightarrow \lambda_{0.05}^{\text{Si}})]}{\left(\frac{I_{\text{Si}}^{\text{Ge}}}{I_{\text{Si}}^{\text{Si}}} I_{\text{Si}}^{\text{Si}}(2) + I_{\text{Ge}}^{\text{Ge}}(2)\right)} \quad (13)$$

The results indicate that, due to Ge surface segregation during growth, samples with Ge surface concentration (x_s) higher than the bulk Ge concentration were obtained. Note that our experiments exhibit a lower Ge surface segregation than the one measured by Jernigan et al. [23] or predicted by Zheng et al. [24] who found 1 ML of Ge at the surface even for $x = 0.05$. The Ge surface concentration depends on the growth temperature, the growth rate, the thickness and the Ge bulk concentration of the SiGe layers. In our growth conditions about 1 ML of Ge has been segregated during the growth of the 28 nm thick $\text{Si}_{0.8}\text{Ge}_{0.2}$ layer ($x_s = 0.81$). This explains the quasi superimposition of the TD-AES peaks of the two $\text{Si}_{1-x}\text{Ge}_x$ layers with $x = 0.2$ and 1 and their close activation energies of desorption.

Fig. 4 shows the variation of the Sb desorption energy (E_d) versus the Ge surface concentration (x_s) measured by AES. From $x_s \sim 0.2$ to 1, E_d varies linearly with x_s displaying the direct relationship between the Sb monolayer desorption temperature and the concentration of Ge atoms segregated to the surface. As previously stated, surface segregation being a homogeneous process for two completely miscible elements, a homogeneous Ge distribution is expected at the surface which can explain the observation of only one desorption peak, and the linear variation of the Sb desorption energy versus x_s for a given adsorption state. This is the case in the range of $0.2 \leq x_s \leq 1$, which illustrates a variation related to a change of

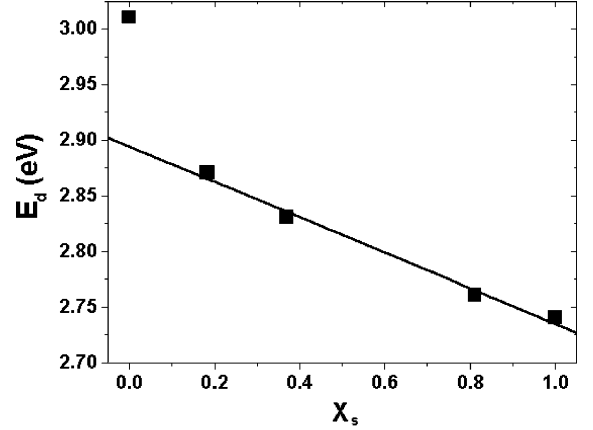


Fig. 4. Sb desorption energy versus the Ge surface composition (x_s) of the SiGe layers measured by AES.

bonding energy but not of adsorption site or adsorption configuration. On the contrary, Fig. 4 shows that in the range of $0 \leq x_s \leq 0.2$ the change of E_d as a function of x_s is abrupt, which can be more easily attributed to a phase transition of the Sb adsorption state (change of adsorption site or adsorption configuration) due to a critical Ge surface concentration (x_s^c). One can notice that this critical Ge surface concentration is close to the percolation threshold (Ge atoms homogeneously distributed on the surface having another Ge atom as a nearest neighbour). x_s^c can be interpreted as the limit between a surface behaviour driven by Si ($0 \leq x_s \leq 0.2$) and a surface behaviour driven by Ge ($0.2 \leq x_s \leq 1$), within each regime a linear variation of the Sb adsorption energy versus the Ge surface concentration. This interpretation is in agreement with the experimental results of Barnett et al. [3] and Chan and Altman [11] who found that the monolayer of Sb desorbs from the Si surface as monomers (Sb_1), and from the Ge surface as dimers (Sb_2). It has been shown that, at low temperature ($T < 600$ °C), the Sb adsorption configuration on both Si(001) [25,26] and Ge(001) surfaces [27–31] is dimers. But calculations [32] evidenced that the Sb–Sb bonding energy of the Sb dimer is lower than the four other Sb–Si bonds which explains the dissociation of the Sb dimers on the Si(001) surface at a lower temperature than the desorption temperature. It was also shown that Sb–Ge bonds are weaker than the Sb–Si bonds,

and that the energy barrier for the dissociation of Sb dimers is lower on Si (0.39 eV/dimer) than on Ge (0.53 eV/dimer) [33]. In consequence, we can expect that the Sb–Sb bond of the Sb dimer on Ge(001) is stronger than the Sb–Ge bonds. This explains why Sb desorbs from the Ge surface as dimers. One can notice that if we extrapolate to $x_s = 0$ the data of Fig. 4 using Eq. (5) for $0.2 \leq x_s \leq 1$, we obtain a Sb dimer adsorption energy equal to 2.89 eV on Si(001), and thus a difference of Sb adsorption energy between Si and Ge, for the dimer configuration, equal to 0.15 eV. This result is in agreement with calculations made by Jenkins and Srivastava [17] who predict that, for the dimer configuration, the Sb–Si bonds are 0.1 eV stronger than the Sb–Ge bonds.

4. Conclusion

AES technique was used to study the Sb thermo-desorption from $\text{Si}_{1-x}\text{Ge}_x$ layers (with $x = 0, 0.05, 0.1, 0.2$ and 1) grown by MBE on Si(100) substrates. We have shown that Sb desorption kinetic from $\text{Si}_{1-x}\text{Ge}_x$ is well described using a first-order reaction and that Sb is less bound to the Ge surface than to the Si one. We quantified by AES the Ge surface segregation which takes place during the growth of the SiGe layers. We have observed two regimes: the first one ($0 \leq x_s \leq 0.2$) where E_d as a function of Ge surface coverage varies rapidly and the second one ($0.2 \leq x_s \leq 1$) where E_d decreases linearly.

Acknowledgements

Thanks are due to A. Saül and G. Tréglia for fruitful discussion and critical reading of the article.

References

- [1] A. Nylandsted Larsen, P. Kringhøj, J. Lundsgaard Hansen, S.Yu. Shiryayev, *J. Appl. Phys.* 81 (1997) 2173.
- [2] K.D. Hobart, D.J. Godbey, M.E. Twigg, M. Fatemi, P.E. Thompson, D.S. Simons, *Surf. Sci.* 334 (1995) 29.
- [3] S.A. Barnett, H.F. Winters, J.E. Greene, *Surf. Sci.* 165 (1986) 303.
- [4] M. Ladevèze, F. Bassani, F. Arnaud d'Avitaya, G. Tréglia, C. Dubois, R. Stuck, *Phys. Rev. B* 56 (1997) 7615.
- [5] A.Yu. Kuznetsov, J. Cardenas, D.C. Schmidt, B.G. Svensson, *Phys. Rev. B* 59 (1999) 7274.
- [6] K. Nakagawa, N. Sugii, S. Yamaguchi, M. Miyao, *J. Cryst. Growth* 201/202 (1999) 560.
- [7] J.R. Power, K. Hinrichs, S. Peters, K. Haberland, N. Esser, W. Richter, *Phys. Rev. B* 62 (2000) 7378.
- [8] C.S. Peng, Q. Thuang, W.Q. Cheng, J.M. Zhou, Y.H. Zhang, T.T. Sheng, C.H. Tung, *Appl. Phys. Lett.* 72 (1998) 2541.
- [9] A. Portavoce, F. Volpi, A. Ronda, P. Gas, I. Berbezier, *Thin Solid Films* 380 (2000) 164.
- [10] R.A. Metzger, F.G. Allen, *Surf. Sci.* 137 (1984) 397.
- [11] L.H. Chan, E.I. Altman, *Phys. Rev. B* 63 (2001) 195309.
- [12] D.A. Grützmacher, K. Eberl, A.R. Powell, B.A. Ek, T.O. Sedgwick, S.S. Iyer, *Thin Solid Films* 225 (1993) 163.
- [13] M. Ladevèze, G. Tréglia, P. Müller, F. Arnaud d'Avitaya, *Surf. Sci.* 395 (1998) 317.
- [14] D.A. Redhead, *Vacuum* 12 (1962) 203.
- [15] S. Andrieu, F. Arnaud d'Avitaya, *Surf. Sci.* 219 (1989) 277.
- [16] R.A. Metzger, F.G. Allen, *J. Appl. Phys.* 55 (1984) 931.
- [17] S.J. Jenkins, G.P. Srivastava, *Phys. Rev. B* 56 (1997) 9221.
- [18] G.G. Jernigan, C.L. Silvestre, M. Fatemi, M.E. Twigg, P.E. Thompson, *J. Cryst. Growth* 213 (2000) 299.
- [19] J. Ushio, K. Nakagawa, M. Miyao, T. Maruizumi, *J. Cryst. Growth* 201/202 (1999) 81.
- [20] G. Tréglia, B. Legrand, F. Ducastelle, A. Saül, C. Gallis, I. Meunier, C. Mottet, A. Senhaji, *Comp. Mater. Sci.* 15 (1999) 196.
- [21] M.P. Seah, W.A. Dench, *Surf. Interf. Anal.* 1 (1) (1979) 2.
- [22] J. Nyéki, Ch. Girardeaux, Z. Erdélyi, G.A. Langer, G. Erdélyi, D.L. Beke, A. Rolland, *Surf. Sci.* 495 (2001) 195.
- [23] G.G. Jernigan, P.E. Thompson, C.L. Silvestre, *Surf. Sci.* 380 (1997) 417.
- [24] Y.-J. Zheng, A.M. Lam, J.R. Engstrom, *Appl. Phys. Lett.* 75 (1999) 817.
- [25] M. Richter, J.C. Woicik, J. Nogami, P. Pianetta, K.E. Miyano, A.A. Baski, T. Kendelewicz, C.E. Bouldin, W.E. Spicer, C.F. Quate, I. Lindau, *Phys. Rev. Lett.* 65 (1990) 3417.
- [26] J. Nogami, A.A. Baski, C.F. Quate, *Appl. Phys. Lett.* 58 (1991) 475.
- [27] M. Lohmeier, H.A. van der Vegt, R.G. van Silfhout, E. Vlieg, J.M.C. Thornton, J.E. Macdonald, P.M.L.O. Scholte, *Surf. Sci.* 275 (1992) 190.
- [28] A. Lessmann, W. Drube, G. Materlik, *Surf. Sci.* 323 (1995) 109.
- [29] N. Takeuchi, *Phys. Rev. B* 55 (1997) 2417.
- [30] G. Falkenberg, L. Seehofer, R.L. Johnson, *Surf. Sci.* 377–379 (1997) 75.
- [31] K. Sumitomo, T. Nishioka, T. Ogino, *Appl. Surf. Sci.* 130–132 (1998) 133.
- [32] S.J. Jenkins, G.P. Srivastava, *Surf. Sci.* 352–354 (1996) 411.
- [33] R.H. Miwa, *Appl. Surf. Sci.* 142 (1999) 52.